Journal of Catalysis 270 (2010) 185–195

Contents lists available at ScienceDirect

Journal of Catalysis

journal homepage: www.elsevier.com/locate/jcat

Effect of zeolite framework type and Si/Al ratio on dimethoxymethane carbonylation

Fuat E. Celik, Tae-Jin Kim, Alexis T. Bell *

Department of Chemical Engineering, University of California, Berkeley, CA 94720, USA

ARTICLE INFO

Article history:
Received 14 November 2009
Revised 22 December 2009
Accepted 25 December 2009
Available online 29 January 2010

Keywords:
Carbonylation
Acid
Zeolite
Faujasite
Carbon monoxide
Formaldehyde
Dimethoxymethane
Methyl methoxyacetate
Ethylene glycol
Disproportionation

ABSTRACT

This work reports on the effects of zeolite framework type and Si/Al ratio on the carbonylation of dimethoxymethane (DMM) to produce methyl methoxyacetate (MMAc). Faujasite (FAU), ZSM-5 (MFI), Mordenite (MOR) and Beta (BEA) showed very similar activity for DMM carbonylation. However, FAU had a very high selectivity to MMAc compared to MFI, MOR and BEA because of very low rates of dimethyl ether (DME) and methyl formate (MF) formation, by-products of the disproportionation of DMM. The high rate of DMM disproportionation observed for MFI, MOR and BEA is ascribed to the small pores of these zeolites, which facilitate a critical initial step in the formation of DME and MF. FER showed very low activity for both carbonylation and disproportionation. Increasing the Si/Al ratio for both FAU and MFI led to an increase in the turnover frequency for DMM carbonylation. It is proposed that the low rate of MMAc formation found at low Si/Al ratios is due to repulsive interactions occurring between adsorbed species located within the same supercage (FAU) or channel intersection (MFI).

1. Introduction

Acid-catalyzed formaldehyde carbonylation has been investigated as a means for producing carbon–carbon bonds for 70 years [1–7]. The products of the reaction, consisting of glycolic acid and its esters and ethers, are desirable as precursors to monoethylene glycol (MEG). This approach to the synthesis of MEG is being pursued because formaldehyde can be produced from synthesis gas-derived methanol [8], a cheaper carbon source than ethene the current starting material for the production of MEG [9]. Fig. 1 shows schemes for synthesizing MEG from formaldehyde and dimethoxymethane (DMM) and demonstrates the equivalence of using formaldehyde and its acetal. Both formaldehyde and DMM are synthesized directly by partial oxidation of methanol [8,10]. The key step in each scheme is the formation of a carbon–carbon bond between formaldehyde/DMM and CO. Coupling carbon monoxide and formaldehyde leads to glycolic acid (GA), whereas the carbonylation of DMM leads to methyl methoxyacetate (MMAc), both of which are precursors to MEG.

Previous investigation of formaldehyde carbonylation has been carried out exclusively in the liquid phase, often requiring carbon monoxide pressures over 100 atm in order to achieve reasonable selectivities [1–6]. In a recent report, we demonstrated for the first time the gas-phase carbonylation of a formaldehyde dialkyl acetal, DMM, over H-Faujasite (H-FAU) [11]. At a CO pressure of 3 atm, 79% selectivity to MMAc could be achieved. Because acetals are often used as protecting groups for aldehydes, this reaction can be considered equivalent to formaldehyde carbonylation. In contrast to liquid-phase carbonylation of formaldehyde, which produces a large number of by-products [2,4,7], the gas-phase carbonylation of DMM involves only two reactions – the carbonylation of DMM to form MMAc and the disproportionation of DMM to form dimethyl ether (DME) and methyl formate (MF).

$$CH_3OCH_2OCH_3 + CO \rightarrow CH_3OCH_2COOCH_3, \quad \Delta G^\circ = -69.0\ \text{kJ mol}^{-1} \quad [12]$$

$$2CH_3OCH_2OCH_3 \rightarrow 2CH_3OCH_3 + HCOOCH_3, \quad \Delta G^\circ = -72.3\ \text{kJ mol}^{-1}$$

The aim of the present investigation was to establish the effects of zeolite framework structure and Si/Al ratio on the gas-phase carbonylation of DMM to MMAc. Experiments were carried out to determine the effects of DMM and CO partial pressures and reaction temperature on the rate of MMAc formation as well. The observed effects of zeolite framework structure and Si/Al ratio are interpreted in the light of a proposed reaction mechanism.

2. Experimental

2.1. Catalyst preparation

Zeolite samples were obtained commercially with different Si/Al ratios in either the NH_4^+ form (NH_4-FAU, Si/Al ≈ 2.6, Si/Al ≈ 6,

* Corresponding author. Fax: +1 510 642 4778.
E-mail address: bell@cchem.berkeley.edu (A.T. Bell).

0021-9517/$ - see front matter © 2009 Elsevier Inc. All rights reserved.
doi:10.1016/j.jcat.2009.12.021

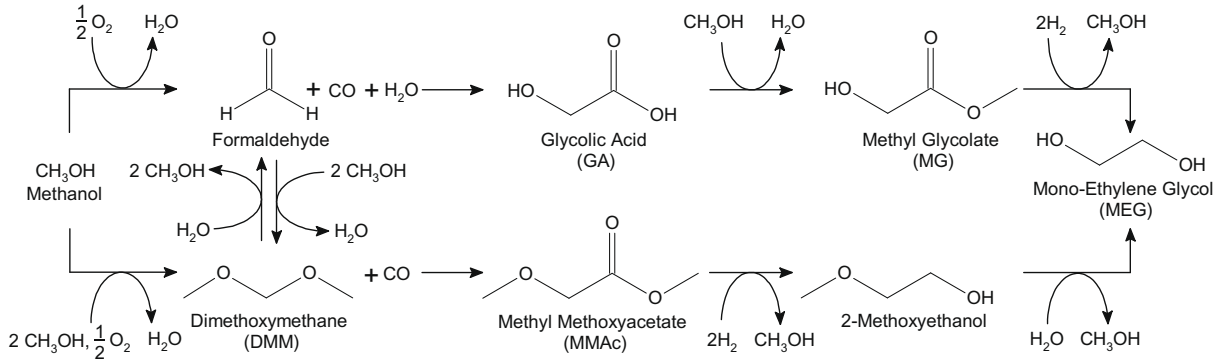

Fig. 1. Scheme for the production of ethylene glycol from methanol via formaldehyde or dimethoxymethane.

Zeolyst; NH_4-MFI, Si/Al ≈ 13.5, Süd-Chemie, Si/Al ≈ 11.5, Si/Al ≈ 15, Si/Al ≈ 25, Si/Al ≈ 40, Si/Al ≈ 140, Zeolyst; NH_4-MOR, Si/Al ≈ 10, Zeolyst; NH_4-BEA, Si/Al ≈ 12.5, Zeolyst; NH_4-FER, Si/Al ≈ 10, Zeolyst) or the H^+ form (H-FAU, Si/Al ≈ 15, Si/Al ≈ 30, Si/Al ≈ 40, Zeolyst). As-received samples were heated to 773 K for 3 h at the rate of 2 K min^{-1} in 100 cm^3 min^{-1} flow of dry air (zero grade) to convert from the NH_4^+ form to the H^+ form and to drive off any adsorbed water. Dried samples were stored in a desiccator prior to use to minimize further adsorption of water.

One sample (Na-MFI, Si/Al ≈ 27.5, Süd-Chemie) was obtained in the Na^+ form and was converted to the NH_4^+ form by aqueous exchange with 1 M NH_4NO_3 solution. 5 g of Na-MFI was exchanged with 0.1 L of solution for 12 h at 353 K three times, filtering and washing with 0.1 L deionized water each time. After the final exchange, the sample was filtered and rinsed again and dried at 383 K for 36 h. Conversion to the H^+ form was achieved by treatment in dry air for 3 h at 773 K as described earlier.

2.2. Steady-state catalytic data

Reactions were carried out in a 6.35 mm OD quartz tube reactor with an expanded section (~12.7 mm OD, ~20 mm length "bubble"). The reactor was packed with quartz wool above and below the catalyst bed to hold the catalyst powder in place. The reactor was placed inside a resistively heated ceramic furnace with external temperature control, and the catalyst bed temperature was measured with a K-type thermocouple sheathed in a quartz capillary placed in direct contact with the bed.

Residual moisture was removed from the catalyst by heating it to 773 K for 3 h at a rate of 2 K min^{-1} in 100 cm^3 min^{-1} flow of dry air. Samples were then cooled to the desired reaction temperature.

CO (99.99% pure research grade, Praxair) was bubbled through a stainless steel saturator filled with DMM (99%, Sigma–Aldrich) and chilled to provide the desired vapor pressure. Additional CO or He (99.999% ultra-high purity, Praxair) was mixed with the saturator exit flow to set the desired CO/DMM ratio and the total gas volumetric flow rate. Reaction products were analyzed using an Agilent 6890n GC equipped with a bonded polystyrene–divinylbenzene (HP-PLOT Q) capillary column connected to a flame ionization detector. Experiments at elevated pressure were carried out by throttling a needle valve located downstream from the reactor.

The total gas flow rate in the reactor was maintained at 100 cm^3 min^{-1} at the reaction pressure, resulting in a gas flow rate between 100 and 300 cm^3 min^{-1} at STP. Since the active centers for carbonylation of DMM are Brønsted-acids sites and the concentration of these sites is proportional to the Al content in a given zeolite, reactor space time was calculated on the basis of the number of moles of Al contained in a given zeolite. Using this definition, space time was varied by choosing the weight of catalyst loaded.

Selectivities to MMAc from DMM are reported based on moles of carbon in MMAc that originated from DMM and were calculated as $S_{MMAc} = \frac{3r_{MMAc}}{2r_{DME}+2r_{MF}+3r_{MMAc}}$, where r_i is the rate of formation of each product i in molar units. Note that only three atoms of carbon in MMAc are derived from DMM, and the fourth carbon atom is derived from CO.

3. Results

3.1. Effect of zeolite framework type

Fig. 2 shows the effect of zeolite framework type on the steady-state rates of MMAc formation (Fig. 2a), DME, and MF formation (Fig. 2b), MMAc selectivity from DMM (Fig. 2c), and DMM conversion (Fig. 2d) as functions of reaction temperature. Zeolites of similar Si/Al ratios were chosen, and the space time was fixed based on moles of Al in the sample at ~0.8 mmol Al min L^{-1}. The partial pressures of CO and DMM in the feed gas were fixed at 1.98 atm and 0.02 atm, respectively.

The dependence of the MMAc formation rate with temperature was complex and depended on zeolite framework type. The MMAc rate showed a maximum with temperature over each zeolite, but the temperature of the maximum rate depended on the zeolite structure. MOR and BEA possessed higher activity to MMAc than FAU and MFI at temperatures in the range of 363–393 K, whereas FAU and MFI possessed higher activity to MMAc than MOR and BEA at higher temperatures in the range of 393–433 K. FER was almost completely inactive but also showed increasing activity to MMAc formation at higher temperatures. The maximum MMAc formation rates observed for FAU, MFI, MOR and BEA were roughly comparable, varying only by a factor of two from each other.

DME and MF formation rates also showed a dependence on zeolite framework type. The rates of both DME and MF formation increased monotonically with temperature, except for the MF formation rate over MOR as discussed in the following paragraphs. MOR and BEA showed very high disproportionation rates that increased almost linearly with temperature above 353 K. The rate of DMM disproportionation was low for MFI up to 393 K and then rose rapidly at higher temperatures such that DME and MF formation rates exceeded those over MOR and BEA at 453 K. By contrast, FAU and FER showed very low, albeit increasing, disproportionation rates at all temperatures.

The ratio of DME to MF was approximately two in most cases, as expected from the stoichiometry of DMM disproportionation. The DME/MF ratio exceeded two at higher temperatures over all zeolite types tested here, except over FAU, where it remained near two, up to 453 K. The deviation from a DME/MF ratio of two was most

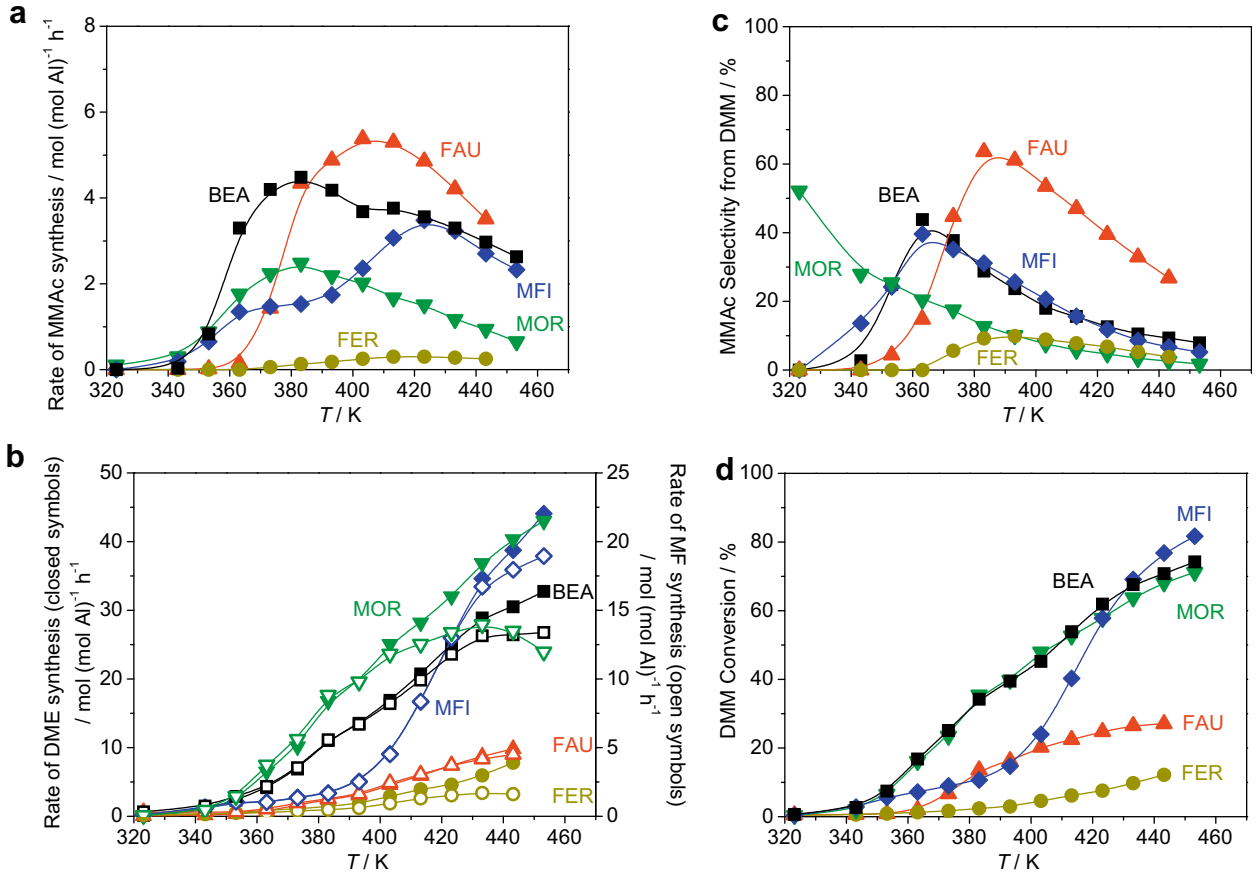

Fig. 2. The effect of reaction temperature over FAU (Si/Al ≈ 15), MFI (Si/Al ≈ 13.5), MOR (Si/Al ≈ 10), BEA (Si/Al ≈ 12.5) and FER (Si/Al ≈ 10) on the rates of (a) MMAc and (b) DME and MF formation, (c) selectivity of MMAc from DMM, and (d) DMM conversion. 0.05–0.08 g catalyst, τ = 0.76–0.86 mmol Al min L^{-1}, P_{CO} = 1.98 atm, P_{DMM} = 0.016–0.019 atm, total gas flow rate = 100 cm^3 min^{-1} at pressure, 200 cm^3 min^{-1} at standard temperature and pressure (STP).

apparent over MOR, where the deviation from two began at lower temperature (403 K) and reached a greater value (DME/MF = 3.6 at 453 K) than for the other zeolites. BEA, MFI and FER showed a significant deviation from a DME/MF ratio of two only above 433 K. The deviation from DME/MF = 2 over MOR was so severe that the MF formation rate decreased with temperature above 433 K. The deviation in the DME/MF ratio from a value of two is attributed to methyl formate decomposition and subsequent dehydration of methanol, as shown below. Taken together, these two reactions could cause a significant increase in the DME/MF ratio.

$$HCOOCH_3 \rightarrow CO + CH_3OH, \quad \Delta G^\circ = +0.4 \text{ kJ mol}^{-1}$$

$$2CH_3OH \rightarrow CH_3OCH_3 + H_2O, \quad \Delta G^\circ = -16.6 \text{ kJ mol}^{-1}$$

At temperatures above 423 K, experiments carried out over MOR showed very small quantities of methyl acetate formation. Methyl acetate arises from the carbonylation of DME [13–15].

$$CH_3OCH_3 + CO \rightarrow CH_3COOCH_3, \quad \Delta G^\circ = -77.0 \text{ kJ mol}^{-1}$$

Methyl acetate was not observed as a product over any of the other zeolites, consistent with observations that MOR catalyzes DME carbonylation more effectively than the other zeolites studied here.

MFI and BEA showed very similar trends in selectivity to MMAc from DMM (Fig. 2c), reaching a maximum selectivity of 40–45% at 363 K. MOR did not show a maximum in selectivity to MMAc, but rather a monotonically declining selectivity with increasing temperature. The high selectivity of MOR at low temperature coincided with a very low MMAc synthesis rate. FAU showed significantly higher selectivity to MMAc than the other zeolites, up to 64% at 383 K, and the temperature range of high selectivity coincided with that for which the rate of MMAc formation was also high. The high selectivity of FAU relative to other zeolites was due partly to its higher MMAc rate, but even more important was its very low rate of DME and MF.

Because of its high selectivity to MMAc and low disproportionation rates at all temperatures, the conversion over FAU was lower than over BEA and MOR at all temperatures, and lower than that over MFI at temperatures above 403 K. The conversion over MFI showed a rapid increase at temperatures above 393 K, coinciding with the increase in the disproportionation rate.

The selectivity to MMAc from CO was 100% for all zeolites. In the few cases where DME carbonylation to methyl acetate occurred over MOR, methyl acetate formation had a negligibly small impact on the selectivity from CO.

Fig. 3 shows the effect of zeolite framework type on the rate of MMAc formation (Fig. 3a) and DME and MF formation (Fig. 3b) as functions of time on stream for FAU, MFI and MOR at 383 K. Zeolites of similar Si/Al ratios were chosen, and the space time was fixed based on moles of Al in the sample at ~0.8 mmol Al min L^{-1}. The partial pressures of CO and DMM in the feed gas were fixed at 1.98 atm and 0.02 atm, respectively.

Over FAU and MFI, the rate of MMAc formation increased initially, reached a maximum value, and then declined slightly and stabilized at a steady value as a function of time on stream. Steady values were reached after about 150 min of exposure to the reaction mixture. Over MOR, the MMAc formation rate also increased for short times on stream, but continued to decrease up to at least

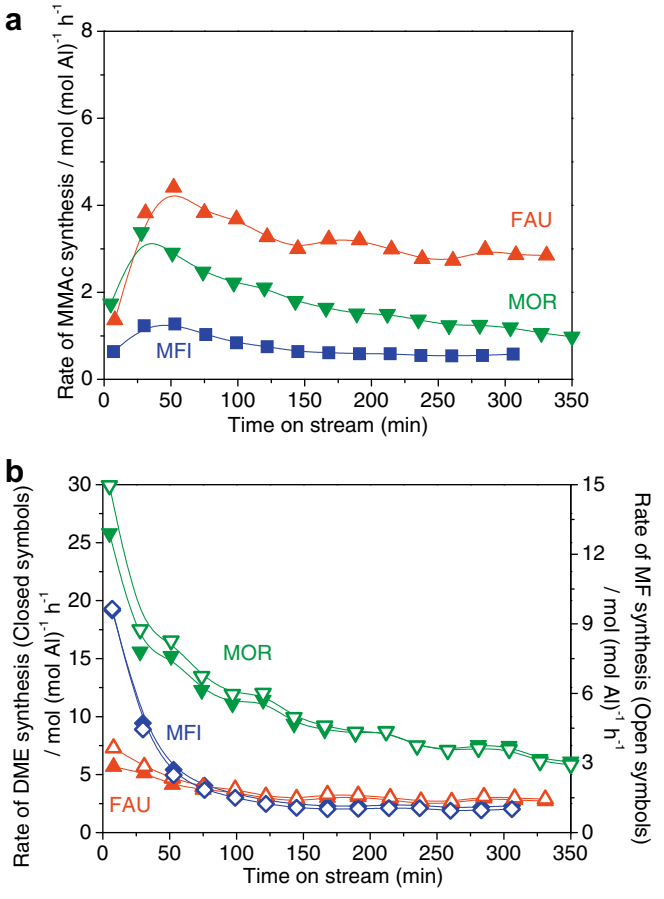

Fig. 3. The effect of time on stream over FAU (Si/Al ≈ 15), MFI (Si/Al ≈ 13.5) and MOR (Si/Al ≈ 10) on the rates of (a) MMAc and (b) DME and MF formation. 0.05–0.08 g catalyst, τ = 0.76–0.81 mmol Al min L^{-1}, T = 383 K, P_{CO} = 1.98 atm, P_{DMM} = 0.013–0.017 atm, total gas flow rate = 100 cm^3 min^{-1} at pressure, 200 cm^3 min^{-1} at STP.

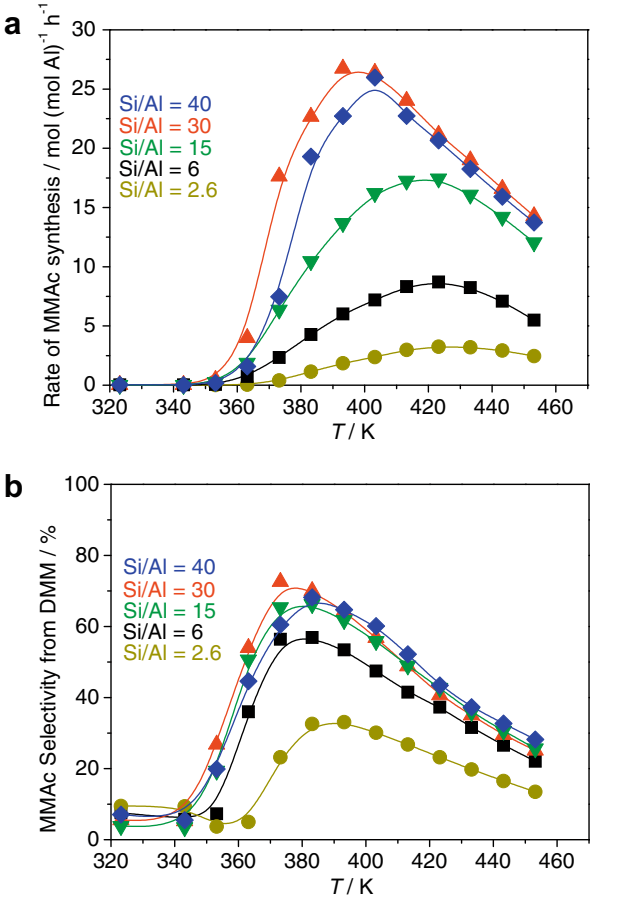

Fig. 4. The effect of reaction temperature over FAU (Si/Al ≈ 2.6–40) on (a) the rate of MMAc formation and (b) selectivity of MMAc from DMM. 0.006–0.07 g catalyst, τ = 0.26–0.28 mmol Al min L^{-1}, P_{CO} = 1.98 atm, P_{DMM} = 0.016–0.017 atm, total gas flow rate = 100 cm^3 min^{-1} at pressure, 200 cm^3 min^{-1} at STP.

350 min. The DME and MF formation rates were initially high over all zeolites at short times on stream. As with MMAc, the DME and MF formation rates reached a steady state after 150 min over FAU and MFI and continued to decrease up to at least 350 min over MOR. After 50 min, selectivity was constant over all three zeolites.

Discrepancies between the steady-state values shown in Fig. 2 and the transient data shown in Fig. 3 can be attributed to the slightly different partial pressures of DMM used in the two types of experiment. The effect of DMM partial pressure can be seen in Fig. 7 and is discussed below.

3.2. Effect of Si/Al ratio over FAU and MFI

Fig. 4 shows the effect of the Si/Al ratio of FAU on the rate of MMAc formation (Fig. 4a) and MMAc selectivity from DMM (Fig. 4b) at steady state for different reaction temperatures. FAU was selected because of the higher activity and selectivity toward MMAc seen for the Si/Al ≈ 15 sample shown in Fig. 2. The partial pressures of CO and DMM in the feed gas were fixed at 1.98 atm and 0.02 atm, respectively. The space time was fixed based on moles of Al in the sample at ~0.27 mmol Al min L^{-1}.

Increasing the Si/Al ratio from 2.6 to 30 increased the MMAc formation rate at temperatures above 363 K. Increasing the Si/Al ratio from 30 to 40 did not increase the rate of MMAc formation any further. The temperature at which the maximum rate was observed shifted to lower values as the Si/Al ratio was increased.

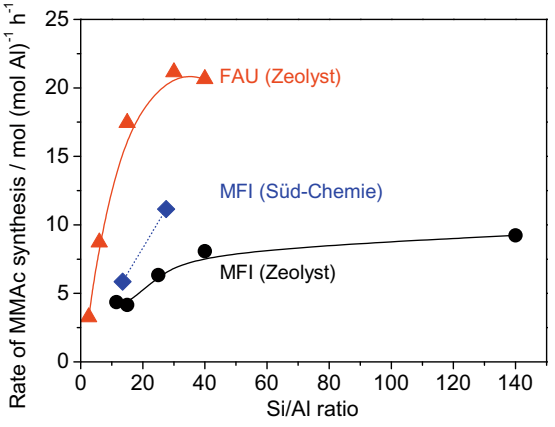

Fig. 5. The effect of Si/Al ratio over FAU (Si/Al ≈ 2.6–40) and MFI samples from two different commercial suppliers (Süd-Chemie, Si/Al ≈ 13.5, 27.5; Zeolyst Si/Al ≈ 11.5–140) on the rate of MMAc formation. 0.006–0.25 g catalyst, τ = 0.26–0.31 mmol Al min L^{-1}, T = 423 K, P_{CO} = 1.98 atm, P_{DMM} = 0.011–0.019 atm, total gas flow rate = 100 cm^3 min^{-1} at pressure, 200 cm^3 min^{-1} at STP.

The rate of DME and MF formation also increased with increasing Si/Al ratio up to 30, beyond which the rates did not increase any further upon increasing the Si/Al ratio to 40. The similarity of the effects of the Si/Al ratio on MMAc and disproportionation

rates caused the selectivity to vary little over samples with different Si/Al ratios. The selectivities for a Si/Al ratio of 6 were only slightly lower than those for Si/Al ratios of 15, 30 and 40. The experiment using a Si/Al ratio 2.6 showed significantly lower selectivity than the other samples.

Increasing the Si/Al ratio of MFI also increased the rate of MMAc formation. Fig. 5 compares the effect of Si/Al ratio on the rates of MMAc formation at 423 K over FAU and over MFI obtained from two different commercial suppliers, Süd-Chemie and Zeolyst. For similar Si/Al ratios, the activities of MFI samples from Süd-Chemie were higher than those obtained from Zeolyst. As with FAU, the MFI samples from Zeolyst showed that increasing the Si/Al ratio increased the MMAc formation rate up to a point, beyond which increasing the Si/Al ratio further showed little improvement. For FAU, this occurred at a Si/Al ratio ≈30, and for MFI the Si/Al ratio was ≈40.

3.3. Effect of reaction conditions over FAU and MFI

The effects of CO partial pressure (P_{CO}), DMM partial pressure (P_{DMM}) and space time (τ) on the reaction rates and selectivities were investigated for FAU (Si/Al ≈ 30) and MFI (Si/Al ≈ 27.5), at a fixed temperature of 383 K.

MFI was chosen for the comparison with FAU because like FAU, it showed a low DMM disproportionation rate at lower temperatures, but unlike FAU, it showed very high disproportionation rates at higher temperatures. This led to high selectivities to MMAc at lower temperatures over MFI, in contrast to the high selectivities to MMAc observed at higher temperatures over FAU. At the chosen temperature of 383 K, the disproportionation rate could still be considered low.

The effect of P_{CO} on the MMAc rate over FAU and MFI is shown in Fig. 6a, the effect on DME rate is shown in Fig. 6b, the effect on MMAc selectivity from DMM is shown in Fig. 6c, and the effect on DMM conversion is shown in Fig. 6d. The partial pressure of DMM in the feed gas was fixed at 0.02 atm, and the space time was fixed at ~0.27 mmol Al min L^{-1}.

Increasing the partial pressure of CO increased the rate of MMAc formation over both FAU and MFI. Both catalysts showed almost linear increases in the rate of MMAc formation with increasing P_{CO} up to 2 atm, followed by slightly slower increases at higher partial pressures. The rate of disproportionation showed almost no dependence on carbon monoxide pressure over FAU, even at zero carbon monoxide pressure, increasing only slightly with increasing P_{CO}. Over MFI, the disproportionation rate showed a very strong dependence on P_{CO}, decreasing rapidly from a very high rate of DME formation at zero carbon monoxide pressure to a moderate rate at 0.2 atm of CO and then continuing to decrease more gradually. Despite the difference in trends, both FAU and MFI showed similar rates of DME formation for CO partial pressures between 1 and 2.5 atm.

The selectivity to MMAc increased monotonically over both zeolites with increasing P_{CO}. The selectivity over FAU increased due to the increasing rate of MMAc formation. The near-constant disproportionation rate caused the rate of increase in the selectivity to decrease with increasing P_{CO}, leveling out near 75%. Over MFI, the increase in selectivity to MMAc was mainly due to the decrease in the rate of DMM disproportion. While the MMAc formation rate

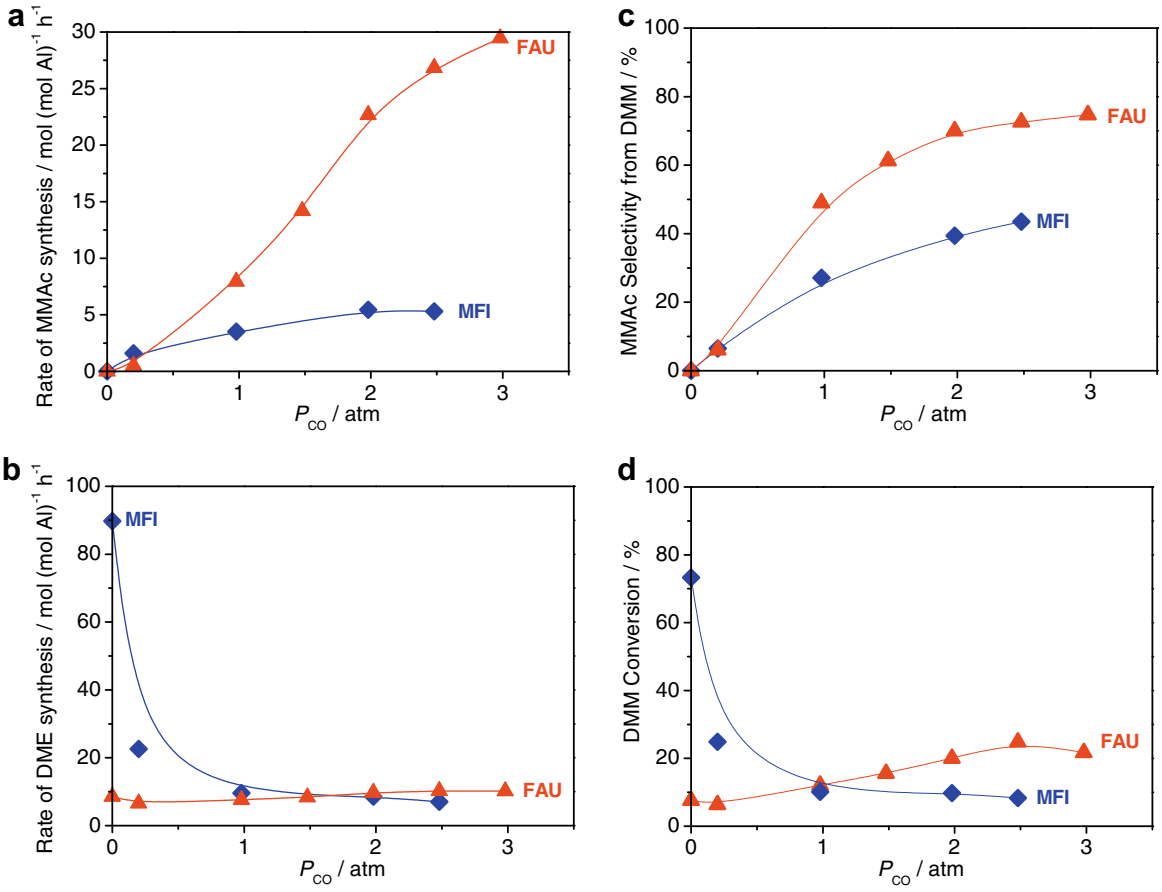

Fig. 6. The effect of CO partial pressure over FAU (Si/Al ≈ 30) and MFI (Si/Al ≈ 27.5) on the rates of (a) MMAc and (b) DME and MF formation, (c) selectivity of MMAc from DMM, and (d) DMM conversion. 0.05 g catalyst, τ = 0.27–0.29 mmol Al min L^{-1}, T = 383 K, P_{DMM} = 0.013–0.019 atm, total gas flow rate = 100 cm^3 min^{-1} at pressure, 100–300 cm^3 min^{-1} at STP.

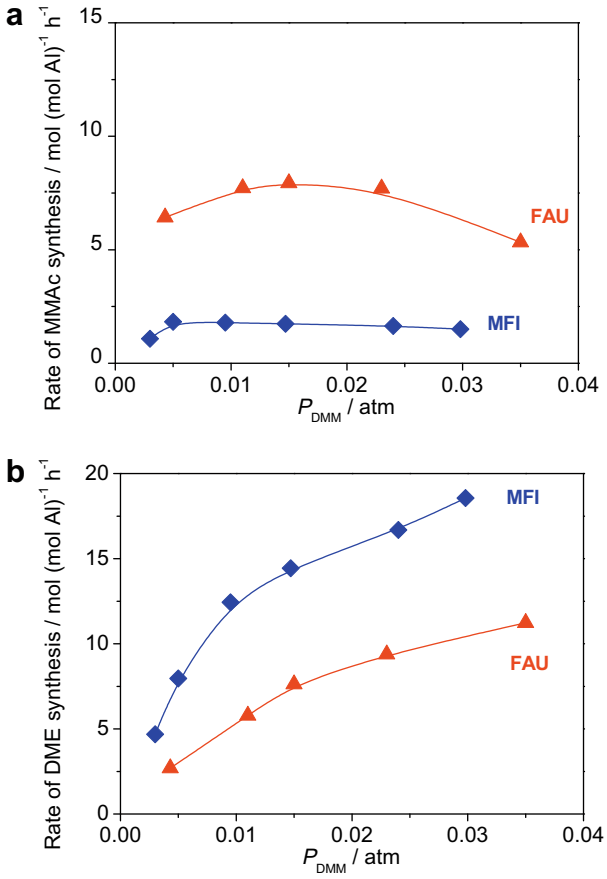

Fig. 7. The effect of DMM partial pressure over FAU (Si/Al ≈ 30) and MFI (Si/Al ≈ 27.5) on the rates of (a) MMAc and (b) DME and MF formation. 0.05 g catalyst, τ = 0.27–0.29 mmol Al min L^{-1}, T = 383 K, P_{CO} = 1.0 atm, P_{He} = 0.97–1.0 atm, total gas flow rate = 100 cm^3 min^{-1} at pressure, 200 cm^3 min^{-1} at STP.

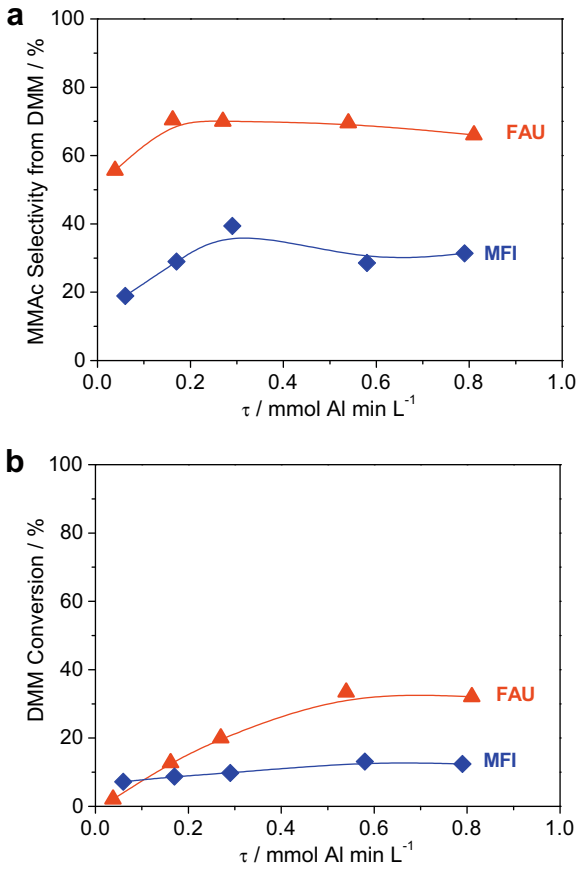

Fig. 8. The effect of space time over FAU (Si/Al ≈ 30) and MFI (Si/Al ≈ 27.5) on (a) selectivity of MMAc from DMM and (b) DMM conversion. 0.007–0.15 g catalyst, T = 383 K, P_{CO} = 1.98 atm, P_{DMM} = 0.015–0.019 atm, total gas flow rate = 100 cm^3 min^{-1} at pressure, 200 cm^3 min^{-1} at STP.

also increased with increasing P_{CO}, this increase was small compared to the decrease in the DME/MF formation rates. The different causes for the observed selectivity increases over FAU and MFI were reflected in the conversion as a function of CO pressure: the overall conversion of DMM increased with P_{CO} over FAU as the MMAc rate increased, whereas the overall conversion of DMM decreased with P_{CO} as the DME formation rate decreased.

The effect of varying DMM partial pressure (P_{DMM}) on the rate of MMAc synthesis (Fig. 7a) and the rate of DME synthesis (Fig. 7b) was compared over FAU and MFI. The reaction temperature was fixed at 383 K, the partial pressure of CO in the feed gas was fixed at 0.98 atm, and the space time was fixed at ~0.27 mmol Al min L^{-1}.

The rate of MMAc synthesis was nearly independent of DMM partial pressure for both FAU and MFI over the range of 0.003–0.035 atm. In the case of FAU, the rate of MMAc formation showed a shallow maximum, whereas for MFI the rate of MMAc formation showed very little change with DMM partial pressure above 0.005 atm after an initial increase between 0.003 and 0.005 atm. The disproportionation rate increased monotonically with P_{DMM}, exhibiting very similar trends for both FAU and MFI.

The space time, τ, of the reaction was varied at a fixed temperature (383 K), P_{CO} (1.98 atm) and P_{DMM} (0.02 atm), over FAU and MFI by varying the amount of catalyst used in the experiment. The effect of τ on MMAc selectivity from DMM is shown in Fig. 8a, and the effect on DMM conversion is shown in Fig. 8b.

Both zeolites showed similar selectivity trends with increasing space time, with the selectivity of DMM to MMAc increasing at short space times and then remaining relatively constant for space times above 0.2 mmol Al min L^{-1}. Conversion of DMM increased with increasing space time over both zeolites, albeit much more slowly over MFI. With selectivity nearly constant as a function of space time, higher yields could be achieved by increasing the space time.

4. Discussion

4.1. Proposed reaction mechanism

The effects of framework type and Si/Al ratio on the activity and selectivity of zeolites to the carbonylation of DMM are best discussed in the context of the proposed reaction mechanism shown in Fig. 9. The first step (Reaction 1) in this scheme is the reaction of DMM with the Brønsted acidic protons of the zeolite (species H-Z), which leads to the formation of methoxymethyl species (MM-Z). The methanol released in this manner is either flushed from the reactor or dehydrated to form DME and water in a manner consistent with the mechanism for DME carbonylation [14]. Recent IR studies in our laboratory have confirmed that upon first exposure of H-FAU or H-MFI to DMM, all Brønsted-acid protons are replaced by methoxymethyl species, a process that is accompanied by the transient formation of methanol.

The methoxymethyl species MM-Z can react with CO (Reaction 2) to form methoxyacetyl species (MA-Z), which can then undergo methoxylation by DMM (Reaction 3), to release MMAc and regenerate the methoxymethyl species. DMM disproportionation is

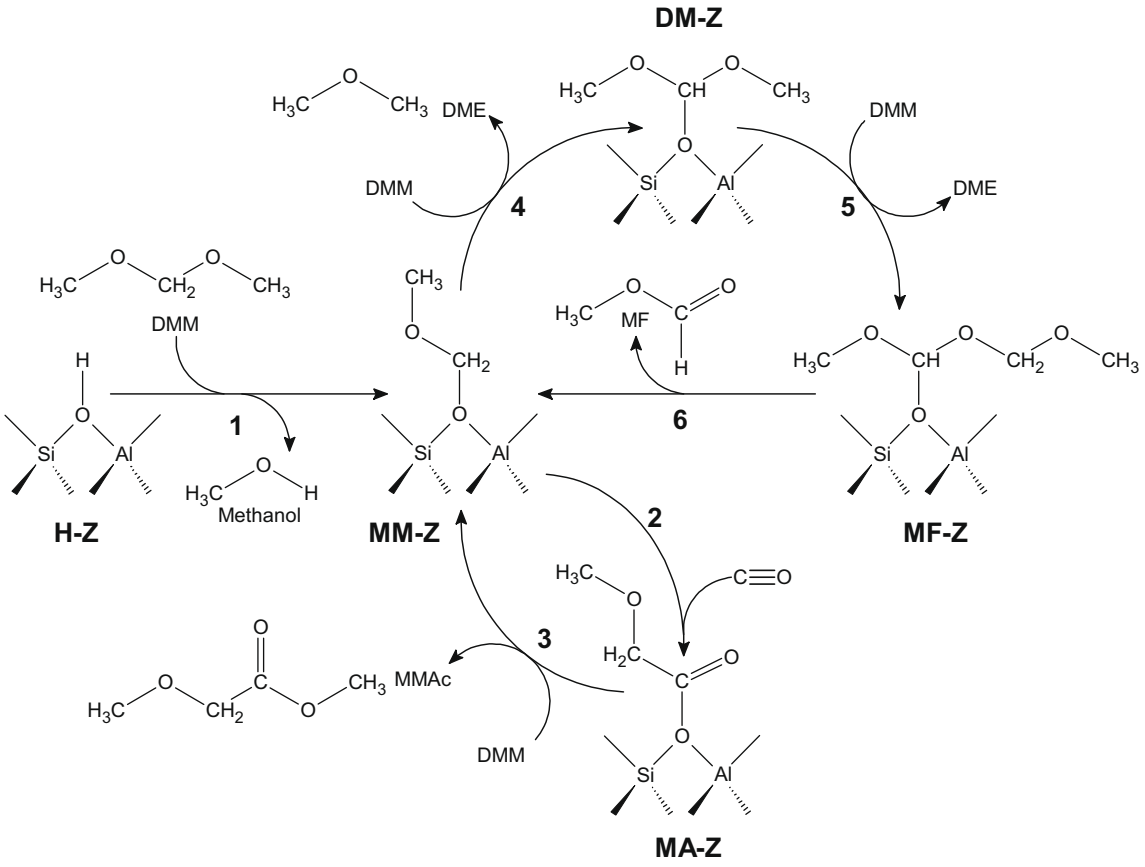

Fig. 9. Proposed reaction mechanism.

envisioned to proceed via reaction of methoxymethyl species with DMM to form dimethoxymethyl species (DM-Z) and DME (Reaction 4). These newly formed surface species can then react with DMM to release a second molecule of DME and a new surface species (MF-Z) (Reaction 5), which decomposes to release MF and regenerate the methoxymethyl species (Reaction 6).

It is thought that MMAc synthesis occurs by the Koch mechanism [2,4,16]. The initiation (Reaction 1) and MMAc synthesis (Reactions 2 and 3) mechanisms proposed here are consistent with those proposed for similar Koch carbonylation reactions [14,17,18]. As formaldehyde disproportionation occurs by the Cannizzaro reaction [19–21], the first step (Reaction 4) of the DMM disproportionation mechanism (Reactions 4–6) proposed here is similar to that for the Cannizzaro reaction of formaldehyde in the liquid phase catalyzed by strong acids [21].

The mechanism proposed in Fig. 9 shows that at steady state methoxymethyl species can undergo carbonylation or disproportionation and that the relative partial pressures of CO and DMM will control the selectivity between these competing reactions. Increasing P_{CO} increases the rate of carbonylation as methoxymethyl species are converted to methoxyacetyl species in Reaction 2. Increasing P_{DMM} increases the disproportionation rate as methoxymethyl species are converted to dimethoxymethyl species in Reaction 4.

Surface methyl groups were excluded from the mechanism due to the very high activation barrier to their formation [22] and are thought to be generally absent from the reaction system considered here. The only exception may be on MOR at higher temperatures, where the formation of surface methyls may explain the observed formation of methyl acetate [13–15]. MOR may possess a greater ability to stabilize surface methyls compared to other zeolites [23], which may in turn promote MF decomposition, which was much more prevalent over MOR than any other zeolite.

4.2. Effect of zeolite framework type

Although the rates of MMAc formation were comparable over FAU, MFI, MOR and BEA (see Fig. 2a), varying by roughly a factor of two, the selectivity to MMAc was much greater over FAU than the other three zeolites (Fig. 2c). This was due to the very low rate of DMM disproportionation observed over FAU.

Of the three proposed steps of the disproportionation rate, the hydrogen-transfer step (Reaction 4) is most likely to be the rate-determining step over the P_{DMM} range studied here. The disproportionation rate was observed to depend on P_{DMM}, meaning that the unimolecular decomposition in Reaction 6 cannot be rate-determining, and methoxyl exchanges, such as in Reaction 5, are generally considered to be fast [14].

The hydrogen-transfer step probably begins with coordination of the nucleophilic oxygen in gas-phase DMM with the bound methoxymethyl species (MM-Z) as shown in Fig. 10. Interaction

Table 1
Pore size [25] and pore dimensionality of different zeolite framework types.

Framework type	T-atoms in pore rings	Maximum included sphere diameter (Å)	Pore dimensionality
FER	10 × 8	6.25	2-D
MFI	10 × 10	6.30	3-D
BEA	12 × 12	6.62	3-D
MOR	12 × 8	6.64	1-D
FAU	12	11.18	3-D

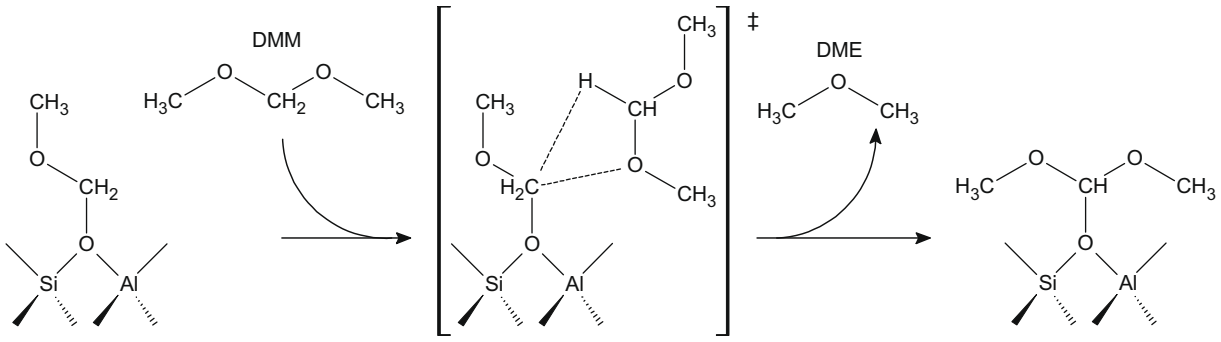

Fig. 10. Proposed transition state for the rate-determining step of DMM disproportionation, illustrating the hydrogen-transfer step.

between DMM and surface methoxymethyl groups is expected to be similar to the interaction between DME and surface methyl groups as described in [23]. After coordination, in order for hydrogen-transfer to occur, the methylene hydrogens on the central carbon of DMM must rotate and face the carbon atom of the methoxymethyl species. If the C–H bond of DMM comes close enough to the adsorbed species, the hydrogen can transfer to the nearby carbon, forming DME from the former species, and replacing it with the new dimethoxymethyl carbocation (DM-Z). The rotated C–H bond of DMM in the hydrogen-transfer step is highlighted as the proposed transition state in Fig. 10.

Since zeolites with Si/Al ratios >10 are generally considered to possess the same acidity regardless of framework type [24], zeolite acidity cannot explain the observed difference in MMAc selectivity among FAU, MFI, MOR and BEA. As discussed in the following paragraphs, these differences can be ascribed to differences in pore size.

Table 1 shows the maximum included sphere diameters in each zeolite framework type, as defined and calculated by Foster et al. [25]. For reference, the T atom counts (Si or Al) in the major channel systems of each zeolite are also shown. The maximum included sphere is considered the largest hard sphere that would fit within the zeolite framework without overlapping framework atoms or distorting the structure [25]. It is usually located inside channel intersections or cage structures and is stationary. The maximum included sphere is nearly uniform for all of the zeolites except FAU, which can fit a sphere at least 68% larger than any of the other zeolites.

Since disproportionation rates were high when the zeolite pore sizes were small, i.e. for MFI, MOR and BEA (Fig. 2b), we propose that the small pores of these zeolites helped to promote the transfer of hydrogen in the transition state shown in Fig. 10. Conversely, the large pores of FAU led to low disproportionation rates by disfavoring the hydrogen-transfer step.

Fig. 11a shows, using MFI as an example, a molecule of DMM interacting with the methoxymethyl species MM-Z in a zeolite possessing smaller pores. Fig. 11b shows a similar interaction in the larger pores of FAU. In the former case, it is seen that the steric constraint of the pore walls forces the hydrogen donor into an orientation that is likely to promote hydrogen-transfer. By contrast, the large pores of FAU allow the hydrogen donor to remain far from the acceptor, so that the driving force for hydrogen-transfer is not as strong.

If CO insertion (Reaction 2) is the rate-determining step in the formation of MMAc, then both carbonylation and disproportionation involve interactions of gas-phase molecules with the methoxymethyl species MM-Z. However, since CO is much smaller than DMM, this interaction is expected to be much less sensitive to spatial constraints than that for the first step in DMM disproportionation (Reaction 4). For this reason, the rate of MMAc formation was almost uniform for FAU, MFI, MOR and BEA (Fig. 2a), while the disproportionation rate was strongly dependent on the pore size of the zeolite (Fig. 2b).

Zeolite dimensionality is believed to play a role in the stability of the different zeolites tested as a function of time on stream. It is generally considered that 1-D and 2-D zeolites are susceptible to deactivation by pore blocking, causing a portion of the catalyst inner surface to become inaccessible [26]. 3-D zeolites are usually

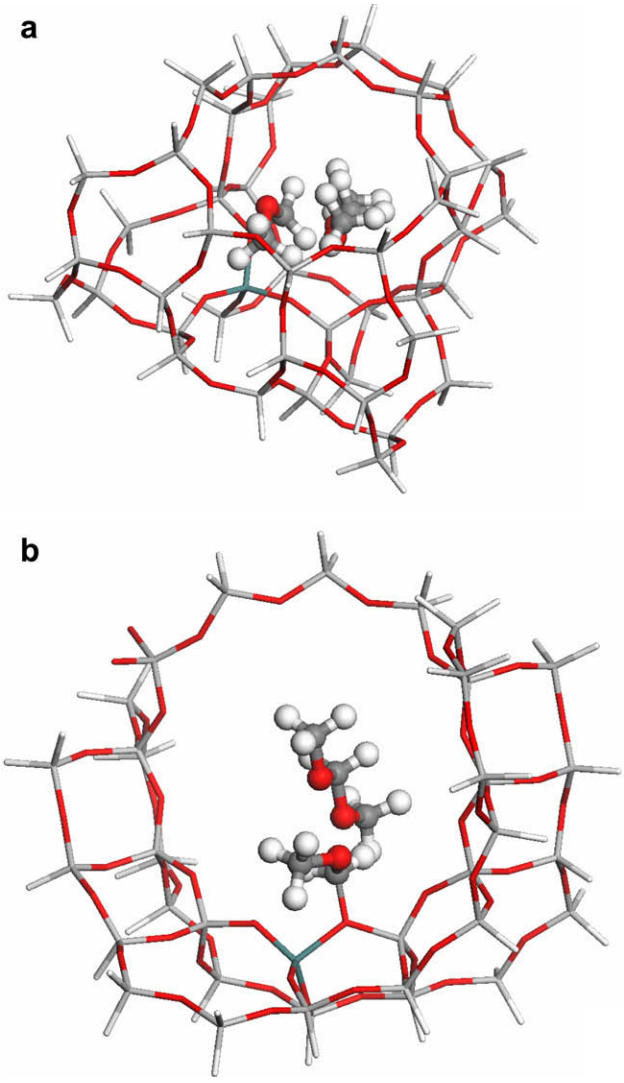

Fig. 11. Illustration of DMM coordinated with surface methoxymethyl species on (a) MFI and (b) FAU.

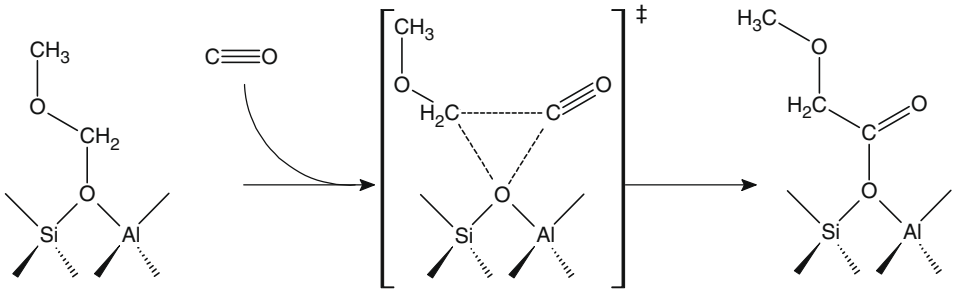

Fig. 12. Proposed transition state for the rate-determining step of DMM carbonylation, illustrating the CO insertion step.

much more stable because all pores are interconnected, and hence pore blockage does not lead to as much loss of access to the catalytically active sites. Fig. 3 shows that FAU and MFI, both 3-D zeolites (Table 1), reached steady-state behavior within 150 min of time on stream, whereas MOR, a 1-D zeolite, continued to decline in activity up to at least 350 min. This difference in time-on-stream behavior may have been a consequence of pore blockage in MOR, which was not a problem in the 3-D zeolites. The low reactivity of FER may also be attributable to its 2-D pore dimensionality. Due to the very low rates of carbonylation and disproportionation, time-on-stream data over FER could not be collected to confirm this projection.

4.3. Effect of Si/Al ratio

Fig. 5 shows that increasing the Si/Al ratio increased the carbonylation rate of DMM per Al over FAU as well as over MFI samples from two different suppliers. Looked at another way, increasing the Al content of the zeolites reduced the rate of MMAc formation. The lower activity of zeolites with Si/Al ratios <10 may be due to lower acidity at each Al center; however, for Si/Al ratios >10, zeolites are considered to have constant acidity as the Al centers are spaced far enough apart to have properties of isolated sites [24]. However, DMM carbonylation rates increased up to Si/Al ratios of ≈30 over FAU and up to ≈40 over MFI.

As mentioned earlier, CO insertion (Reaction 2 in Fig. 9) is likely to be the rate-determining step in the carbonylation mechanism. Fig. 12 illustrates the proposed transition state for this process based on DFT calculations [27]. The methoxymethyl species (MM-Z) dissociates partially from its adsorption site before inserting CO between the methoxymethyl carbon and the framework oxygen atom to form the methoxyacetyl species (MA-Z) [27]. The partial dissociation of the methoxymethyl species produces a cationic transition state, as expected in a Koch carbonylation mechanism [14,16,22,23], and localizes positive charge on the dissociating fragment.

For Si/Al ratios >10, spacing between Al centers is sufficient to have no effect on acidity [24], although surface species adsorbed on these centers may be close enough to interact with each other. Fig. 13 illustrates the distance between two methoxymethyl species if they were located within the same supercage of FAU. A distance of 1.5 Å is typical for carbon-framework oxygen distances in adsorbed species on zeolite surfaces (e.g. [23]). The location of the two Al atoms was chosen as an intermediate distance – some Al–Al pairs lead to longer distances between adsorbed species, while most pairs lead to shorter distances. In this representative example, the distance between methoxymethyl species is only 6.2 Å. Upon the dissociation of one of these species to form the transition state shown in Fig. 12, the distance between species decreases as the positive charge on the dissociating fragment increases. Had the zeolite been drawn with more than two Al atoms in a single supercage, the distances between surface species would have been smaller still.

The distances between dissociated carbocations and neighboring surface species, when less than 6 Å, may be short enough for Coulombic interactions to have an effect. Thus, a carbocation might experience an increase in the activation energy required for

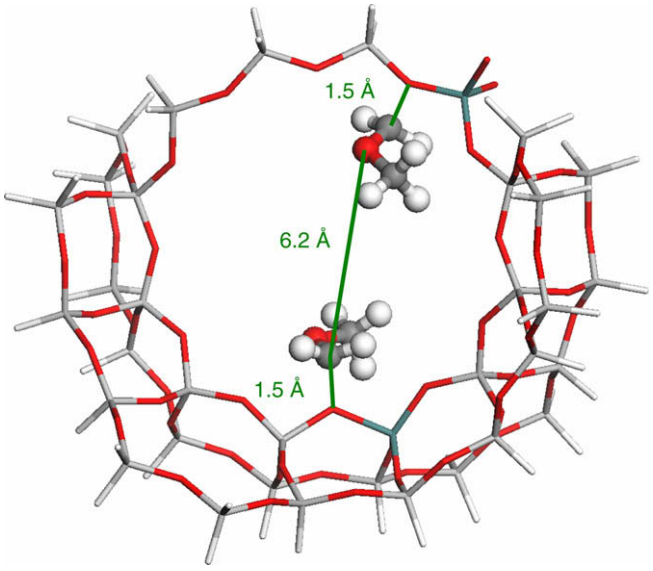

Fig. 13. Illustration of interspecies distances for two methoxymethyl species coordinated to Al atoms within the same supercage of FAU.

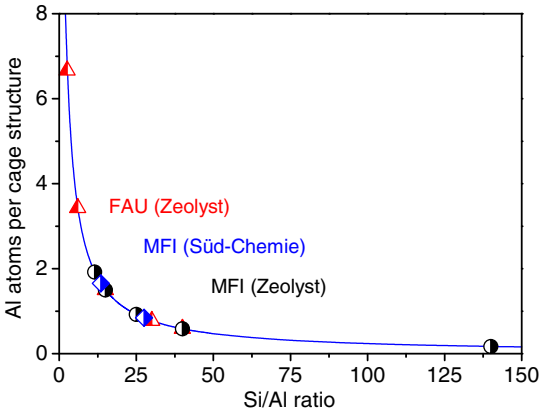

Fig. 14. Calculated average number of Al atoms per cage structure in FAU and MFI samples from Zeolyst and Süd-Chemie of different Si/Al ratios as reported by the suppliers. A cage structure is a supercage in FAU and a channel intersection in MFI. A curve of $24/(1 + R)$, where R is the Si/Al ratio, has been plotted passing through all the points [28].

dissociation due to these repulsive interactions. This would imply that the activation energy should decrease with increasing distance between active sites within a zeolite. Since decreasing the Al content of a zeolite would increase the distance between Al centers, higher Si/Al ratios would be expected to lead to higher reaction rates due to the lower activation barriers. This effect can be seen in Fig. 5 and holds for both FAU and MFI.

Fig. 14 shows the calculated average number of Al atoms in each cage structure of FAU and MFI for each Si/Al ratio shown in Fig. 5 [28]. The supercages of FAU are the cage structures, and in MFI the channel intersections are the cage structures. In Fig. 5, the rate of MMAc synthesis over FAU increased with increasing Si/Al ratio up to a Si/Al ratio of ≈30, which also corresponded to the Si/Al ratio at which there was no more than one Al atom per supercage. This suggests that in FAU, the size of the supercage is roughly the same as the distance at which surface species no longer interact with each other. In MFI, the rate of MMAc synthesis increased up to a Si/Al ratio of ≈40, which corresponded to 0.59 Al atoms per channel intersection. This suggests that one active site for every 1.7 channel intersections is a sufficient distance to avoid interaction between surface species. Note that the largest stationary sphere in FAU, corresponding to the supercage, was 1.8 times larger than the largest sphere in MFI, which corresponds to a channel intersection (see Table 1). This gives a similar estimate for the minimum separation for active sites in both FAU and MFI to avoid interactions between surface species.

The differences between the Süd-Chemie and Zeolyst samples may be the location of the Al atoms in the framework as a function of their synthesis techniques – i.e. samples from Zeolyst may have Al atoms clustered closer together, resulting in more interactions between adsorbed species, while samples from Süd-Chemie may have them more evenly spaced.

4.4. Effect of reaction conditions

The rate of MMAc formation was observed to go through a maximum with temperature, suggesting that the carbonylation mechanism in Fig. 9 is not sufficient to describe the observed kinetics. To explain the maximum, either Reaction 2 or Reaction 3 of the mechanism must be reversible. A maximum in the MMAc formation rate was observed over all zeolite samples tested here, including FER, which gave a maximum at a MMAc partial pressure of 2×10^{-4} atm. As the reversibility was observed even for such low MMAc partial pressures, it is unlikely that Reaction 3 was reversible under the reaction conditions tested here. Therefore, it is likely that Reaction 2 is reversible, at least at higher temperature.

Taken together, the observed effects of P_{CO} and P_{DMM} on the rates of DMM carbonylation and disproportionation indicate slightly different mechanisms over FAU and MFI. DMM carbonylation showed roughly first-order dependence on P_{CO} and zero-order dependence on P_{DMM} over both zeolites (Figs. 6a and 7a). Additionally, DME formation over both FAU and MFI showed less than first-order dependence on DMM pressure (Fig. 7b). However, the two zeolites showed differences in the dependence of DME formation on the partial pressure of CO (Fig. 6b). Over MFI, DME formation showed negative-order dependence on CO pressure. This suggests that over MFI, carbonylation and disproportionation compete with each other as shown in Fig. 9, with methoxymethyl groups undergoing disproportionation if reacting with DMM and undergoing carbonylation if reacting with CO. Over FAU, the rate of DME formation was nearly independent of P_{CO}. This suggests that over FAU, the active sites for disproportionation and carbonylation are somehow distinct, with some methoxymethyl species primarily undergoing carbonylation and some primarily undergoing disproportionation.

It is known that FAU has four distinct positions for the Brønsted acidic proton, corresponding with the four O atoms surrounding each Al atom in the zeolite framework [29]. Of these, only two are theoretically accessible to gas-phase molecules in the zeolite pores, the so-called O(1) site, whose protons point into the supercages of FAU, and the O(4) site, whose protons point toward the ring openings [29]. When the protons are displaced by reaction with DMM (Reaction 1 of Fig. 9), some of the resulting methoxymethyl species may orient themselves at O(4) sites, while the rest would orient themselves at less sterically hindered O(1) sites. The unhindered O(1) sites may be those responsible for carbonylation, while the O(4) sites may undergo disproportionation. This would be consistent with the conclusion from Section 4.2 that more sterically hindered sites promote disproportionation.

5. Conclusions

Of the zeolites tested here, FAU was the most effective catalyst toward DMM carbonylation because of its low disproportionation rates and high carbonylation rates. FAU with a Si/Al ratio of ≈30 has been shown to achieve 79% selectivity to MMAc from DMM at 3 atm of CO pressure, 0.02 atm of DMM pressure and 383 K [11].

The high selectivity of FAU was shown to derive from its large supercages, which disfavor disproportionation. By contrast, the smaller pores of MFI, MOR and BEA force the reactants into an orientation that promote the hydrogen-transfer step critical to disproportionation.

MMAc formation rates over FAU and MFI increased with increasing Si/Al ratio. Low Al zeolites led to higher carbonylation rates because with fewer Al atoms within the zeolite framework, Al centers and the surface species adsorbed on them were spaced farther apart from one another, thereby avoiding repulsive electrostatic interactions between surface species. The closer proximity of surface species in high Al zeolites led to increased activation energies in the cationic transition state of CO insertion step of the carbonylation mechanism.

The effects of P_{CO} and P_{DMM} on the carbonylation rates and the effect of P_{DMM} on the disproportionation rates were similar over both FAU and MFI. By contrast, CO pressure was shown to have a negative effect on disproportionation over MFI, and no effect over FAU. This suggests that while a single active species undergoes both carbonylation and disproportionation over MFI, surface species adsorbed at the O(1) site of FAU are responsible for carbonylation, while those at the O(4) site undergo disproportionation.

Acknowledgments

The authors would like to acknowledge Dr. Vladimir Shapovalov for valuable discussions and for his assistance in preparing images of zeolite framework sections. This work was supported by the Methane Conversion Cooperative funded by BP.

References

[1] D.J. Loder, US Patent 2 152 852 (1939), to E.I. du Pont de Nemours & Co.
[2] D.E. Hendriksen, Prepr. Pap. – Am. Chem. Soc., Div. Fuel Chem. 28 (1983) 176.
[3] H.J. Schmidt, H.J. Arpe, US Patent 4 501 917 (1985), to A.G. Hoechst.
[4] S.Y. Lee, J.C. Kim, J.S. Lee, Y.G. Kim, Ind. Eng. Chem. Res. 32 (1993) 253.
[5] E. Drent, W.P. Mul, B.J. Ruisch, US Patent 6 376 723 (2002), to Shell Oil Company.
[6] T. Li, Y. Souma, Q. Xu, Catal. Today 111 (2006) 288.
[7] F.E. Celik, H. Lawrence, A.T. Bell, J. Mol. Catal. A: Chem. 288 (2008) 87.
[8] K. Ivanov, Appl. Catal. A 116 (1994) L1.
[9] J.M. Berty, Ethylene oxide synthesis, in: B.L. Leach (Ed.), Applied Industrial Catalysis, vol. 1, Academic Press, New York, 1983, p. 207.
[10] J.M. Tatibouet, Appl. Catal. A 148 (1997) 213.
[11] F.E. Celik, T. Kim, A.T. Bell, Angew. Chem. Int. Ed. 48 (2009) 4813.
[12] ΔG° values for reactions were estimated from published ΔG_f° or ΔH_f° and S° values where available [Standard thermodynamic properties of chemical

substances, in: D.R. Lide (Ed.), CRC Handbook of Chemistry and Physics, 88th ed. (Internet Version 2008), CRC Press/Taylor and Francis, Boca Raton, FL, 2008; P.J. Linstrom, W.G. Mallard (Eds.), NIST Chemistry WebBook, NIST Standard Reference Database Number 69 National Institute of Standards and Technology, Gaithersburg, MD, http://webbook.nist.gov, (retrieved March 13, 2008)] or from group contribution theory otherwise [Prediction and correlation of physical properties, in: D.W. Green (Ed.), Perry's Chemical Engineers' Handbook, seventh ed., McGraw Hill, New York, 1997].
[13] P. Cheung, A. Bhan, G.J. Sunley, E. Iglesia, Angew. Chem. Int. Ed. 45 (2006) 1617.
[14] P. Cheung, A. Bhan, G.J. Sunley, D.J. Law, E. Iglesia, J. Catal. 245 (2007) 110.
[15] A. Bhan, A.D. Allian, G.J. Sunley, D.J. Law, E. Iglesia, J. Am. Chem. Soc. 129 (2007) 4919.
[16] H. Bahrmann, Koch reactions, in: J. Falbe (Ed.), New Syntheses with Carbon Monoxide, Springer, Berlin, 1980, p. 372.
[17] A.G. Stepanov, M.V. Luzgin, V.N. Romannikov, V.N. Sidelnikov, K.I. Zamaraev, J. Catal. 164 (1996) 411.
[18] Q. Xu, S. Inoue, N. Tsumori, H. Mori, M. Kameda, M. Tanaka, M. Fujiwara, Y. Souma, J. Mol. Catal. A: Chem. 170 (2001) 147.
[19] J.F. Walker, Formaldehyde, American Chemical Society Monograph Series, Reinhold, London, 1964, p. 214.
[20] Y. Tsujino, C. Wakai, N. Matubayashi, M. Nakahara, Chem. Lett. (1999) 287.
[21] S. Morooka, N. Matubayasi, M. Nakahara, J. Phys. Chem. A 111 (2007) 2697.
[22] Y.J. Jiang, M. Hunger, W. Wang, J. Am. Chem. Soc. 128 (2006) 11679.
[23] M. Boronat, C. Martinez-Sanchez, D. Law, A. Corma, J. Am. Chem. Soc. 130 (2008) 16316.
[24] H.G. Karge, Concepts and analysis of acidity and basicity, in: G. Ertl, H. Knözinger, F. Schüth, J. Weitkamp (Eds.), Handbook of Heterogeneous Catalysis, second ed., Wiley, New York, 2008, p. 1103.
[25] M.D. Foster, I. Rivin, M.M.J. Treacy, O. Delgado Friedrichs, Micropor. Mesopor. Mater. 90 (2006) 32.
[26] K. Yoo, E.C. Burckle, P.G. Smirniotis, J. Catal. 211 (2002) 6.
[27] V. Shapovalov, A.T. Bell, Manuscript inpreparation.
[28] The FAU structure contains 192 T atoms (either Si or Al) per unit cell and 8 supercages per unit cell [G.H. Kühl, Modification of zeolites, in: J. Weitkamp, L. Puppe (Eds.), Catalysis and Zeolites, Springer, Berlin, 1999, p. 89], giving 24 T atoms per supercage. The average number of Al atoms per supercage is then $24/(1+R)$, where R is the Si/Al ratio. The MFI structure contains 96 T atoms and 4 channel intersections per unit cell [B. Millot, A. Méthivier, H. Jobic, H. Moueddeb, J.A. Dalmon, Micropor. Mesopor. Mater. 38 (2000) 85], giving 24 T atoms per channel intersection, so that the average number of Al atoms per channel intersection is also $24/(1+R)$.
[29] K. Schröder, J. Sauer, J. Phys. Chem. 100 (1996) 11043.